Magnetic Proximity Effects in van der Waals Heterostructures

Mireia Tena Zuazolacigorraga

Supervised by: Juan F. Sierra, Sergio O. Valenzuela
Physics and Engineering of Nanodevices

Institut Català de Nanociència i Nanotecnologia. Av. de Serragalliners, 08193 Bellaterra, Barcelona.
July 2022

Motivated by the recent discovery of 2D materials with ferromagnetic order and the continuous advances in the fabrication of artificial van der Waals heterostructures, the experimental work carried out in this master thesis focuses on proximity-induced magnetism in high spin-orbit layered materials. In particular, we have investigated magneto-transport and anomalous Hall effects in the van der Waals system WTe_2/CGT. This is the preliminary step towards the realization of the QAHE, which requires the co-integration of monolayer WTe_2 with a perpendicular magnetized 2D ferromagnet. Our experiments show that AHE is present on our samples, but this key observation is not a definitive proof of proximity-induced magnetism, but due to shunting of the electrical current to the CGT layer with an increased conductivity attributed to doping caused by thermal annealing. We have observed that the doping is also linked to an enhanced anisotropy and Curie temperature of CGT. The findings claim for a thorough revision of recent reports of the AHE induced by CGT in adjacent high spin-orbit materials.

Keywords: 2D materials, van der Waals heterostructures, proximity effects, quantum anomalous Hall effect, anomalous Hall effect.

Mireia Tena Zuazolacigorraga: mireia.tena@icn2.cat

Acknowledgements

Contents

1   Introduction

Owing to the rich variety of physical phenomena and emerging technologies, the synthesis and isolation of two dimensional (2D) materials has become of great interest in the last years. 2D materials can be naturally extracted from a variety of bulk van der Waals materials, and remarkably, isolated atomically thin layers can be reassembled on top of each other into more complex artificial heterostructures. As a result, it is feasible to engineer artificial van der Waals systems combining materials with different physical properties. On another note, the revolution of the topological perspective in material science has sparked intense experimental efforts to observe exotic states of matter such as the Quantum Anomalous Hall effect (QAHE). The QAHE is characterized by the quantization of the Hall conductivity in integer multiples of the von Klitzing constant (e^2/h), and therefore, might have a strong impact in metrology applications.

This master thesis is an experimental work embedded in the first steps towards the realization of the QAHE in van der Waals heterostructures. With that long-term goal, the initial objective of the project is to advance in the understanding of the magnetic proximity effects that can arise in van der Waals heterostructures that combine the 2D layered magnet $Cr_2Ge_2Te_6$ (or CGT) and WTe_2, a high spin-orbit layered material hosting topological properties in the monolayer limit. A device composed of WTe_2 and CGT was fabricated and characterized by magneto-transport measurements, searching for proximity-induced magnetism in WTe_2. We observed that the sample processing caused an unexpected behaviour of the magnetic material that included a notable increase in both magnetic anisotropy and T_c. These results motivated a change of focus to a dedicated study of the properties of CGT, which became the main subject of this thesis. Devices composed solely of the magnetic material were fabricated and characterized, with the objective to gain better understanding of the observed phenomena.

This section includes a brief introduction to van der Waals materials and heterostructures, followed by a presentation of proximity-induced effects for the realization of the Quantum Anomalous Hall effect (QAHE) in van der Waals systems. We continue with an experimental background that presents the most remarkable physical properties of the participating van der Waals materials and explains the use of the anomalous Hall effect (AHE) to detect magnetic order. We begin the experimental part by presenting the fabrication of heterostructures and devices for electrical transport measurements, followed by a detailed description of the measurement setup. The next section presents the results of the magneto-transport measurements in the fabricated devices. Finally, the master thesis is concluded with a presentation of the main experimental findings and the proposal of next experiments.

1.1   Van der Waals materials and heterostructures

Van der Waals layered materials are formed by atomically thin layers held together by van der Waals forces. The interlayer van der Waals interaction is orders of magnitude weaker than the intralayer covalent bonds, which enables the mechanical exfoliation of these materials and the isolation of atomically thin flakes down to the monolayer limit. Since the isolation of graphene by Andrei Geim and Kostantin Novoselov in 2004 the family of van der Waals materials has significantly grown to materials that exhibit insulting, metallic, semiconducting and superconducting behaviours. Very recently, magnetism has also been observed in atomically thin magnetic crystals [GKMN19].

The atomically thin nature of 2D materials enables their co-integration in artificial heterostructures with atomically sharp interfaces. Such heterostructures combine the respec-

tive material properties and, remarkably, enable to imprint properties which are absent in the isolated material through short-range proximity interactions across interfaces [JFS21]. This opens a new perspective for artificial material design based on proximity effects. One example of such phenomena would be the already well established superconducting proximity effect, in which superconducting properties penetrate into an adjacent material over a characteristic length [GPB$^+$96]. The thesis focuses on inducing magnetism in a high spin-orbit layered material when combined with a 2D ferromagnet via a proximity effect.

1.2 Proximity-induced magnetism in Topological Insulators

The emergence of the QAHE requires materials with time reversal symmetry breaking, which can be achieved by means of intrinsic magnetic ordering [WYH$^+$15]. The QAHE is characterized by the presence of dissipationless charge currents at the edges, as schematically shown in Figure 1(b), and anomalous Hall resistance quantization. The effect is similar to the Quantum Hall Effect (Fig. 1(a)), but in absence of an external magnetic field. Since its first theoretical prediction [Hal88], many efforts have been made to experimentally realize the QAHE, but it was not until 2013 when it was observed for the first time at ultra low temperatures (300 mK) in the Magnetic Topological Insulator (MTI) (Bi,Sb)$_2$Te$_3$ doped with Cr [CZF$^+$13] and V [CZK$^+$15]. However, magnetic doping introduces disorder that degrades electronic properties of the material, a thus restricts the observation of the anomalous Hall quantization at ultra low temperatures. An alternative solution to this problem is to look for intrinsic MTIs such as MnBi$_2$Te$_4$ [DYS$^+$20]. However, the emergence of the QAHE on these materials requires a precise control in the number of layers, defects and termination, which is very challenging from the point of view of thin film growth by molecular beam epitaxy techniques [LH21]. To date, the QAHE has been observed in the intrinsic MTI MnBi$_2$Te$_4$ at temperatures below 2K [OKB$^+$19].
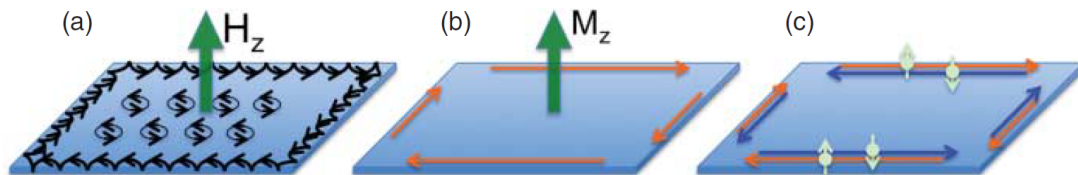
Figure 1: Schematic illustrations of the edge states in (a) QHE, (b) QAHE and (c) QSHE.
Source: Hongming Weng, Rui Yu, Xiao Hu, Xi Dai Zhong Fang (2015) Quantum anomalous Hall effect and related topological electronic states, Advances in Physics, 64:3, 227-282, DOI: 10.1080/00018732.2015.1068524

Another approach towards the realization of the QAHE is to exploit the unique properties of van der Waals heterostructures and proximity-induced effects. Here, the key idea is to combine 2D TIs, such as monolayer 1T'-WTe$_2$, with 2D magnets with perpendicular magnetic anisotropy. 2D TIs host the Quantum Spin Hall Effect (Fig.1(c)), characterized by the presence of pairs of edge states composed of two counter-propagating chiral channels that, in proximity to the 2D magnet, would result in the QAHE. This novel approach is appealing since it avoids the use magnetic doping, and– in principle–provides a platform to observe anomalous Hall quantization at higher temperatures.

Attempts of using the proximity-induced effects have been carried out in systems that combine conventional 3D magnets with 3D TIs as well [BAG$^+$21]. However, the interface between conventional magnets and TIs are far from being ideal, presenting intermixing of materials and alloying, thus creating dead layers. The main advantage of using 2D materi-

als instead, is the atomically sharp interface, which is free of defects and intermixing, and the multiple combinations thanks to the plethora of 2D materials with different physical properties available. This approach is yet in its infancy, and requires a thorough survey of proximity-induced magnetism in van der Waals heterostructures, as well as studying different material combinations. In this regard, the master thesis deals with the investigation of magnetic proximity effects in few layers WTe_2 by adjacent 2D magnet $Cr_2Ge_2Te_6$ (CGT).

2 Experimental background

The aim of this section is to provide the necessary background to understand the magneto-transport experiments carried out. We include a presentation of the employed van der Waals materials WTe_2 and CGT, as well as an introduction to the use of the anomalous Hall effect (AHE) to detect magnetic order.

2.1 Physical properties of the participating materials

2.1.1 Transition metal dichalcogenide WTe_2

WTe_2 belongs to the family of transition metal dichalcogenides (TMDCs), which are semiconductors of the type MX_2, where M is a transition metal atom (such as Mo or W) and X is a chalcogen atom (such as S, Se or Te). TMDCs have drawn attention in the last years because their high spin-orbit coupling properties and optically active nature with high prospects in spintronic and optoelectronic technological applications [MOP$^+$17].

WTe_2 is a type-II Weyl semi-metal [LWH$^+$17], presenting an electronic band structure with electron and hole pockets at the Fermi energy, resulting in the coexistence of electron and hole carriers in the electrical transport [DSC$^+$19]. A variety of novel physical phenomena have been discovered in this material, such as a non-saturating parabolic magnetoresistance up to 16 T [AXF$^+$14], whose physical origin is believed to be related to the perfect balance of electron and hole carriers. In the monolayer limit, it has been experimentally demonstrated that WTe_2 is a 2D TIs [TZW$^+$17] [ZRF$^+$21] in the 1T' phase, which makes it a suitable candidate for the realization of QAHE when proximitized to a magnetic material. We note that realizing the QAHE is not the objective of the master thesis, but to induce magnetism on few-layer WTe_2. The success of the proximity effect would make the WTe_2/CGT heterostructure a potential host for QAHE in future monolayer devices.

Owing to the inherently short-range of the proximity effect, the induced magnetism only affects the first layers of WTe_2 in contact with CGT. For that reason, the WTe_2 has to be thin enough in order maximize the number of layers affected by the adjacent CGT.

2.1.2 Van der Waals ferromagnet $Cr_2Ge_2Te_6$

In two dimensional systems, the long-range magnetic order is strongly suppressed by thermal fluctuations, according to the Mermin–Wagner theorem [MW66]. However, these thermal fluctuations can be counteracted by magnetic anisotropy leading to magnetic order. After the discovery of 2D magnetic materials, the efforts are focused on the isolation and synthesis of 2D magnets with room temperature ferromagnetism. $Cr_2Ge_2Te_6$ (CGT) is a 2D ferromagnetic semiconductor with perpendicular magnetic anisotropy and Curie temperature $T_C = 66K$ [SBW$^+$20]. When subject to small out-of-plane magnetic field, CGT presents perpendicular magnetic anisotropy surpassing its intrinsic magnetocrystalline anisotropy. This magnetic order has been observed down to the bilayer limit with a Curie temperature that varies from T_c=30K for bilayers, gradually increasing up to T_c

=66K for bulk crystals [GLL$^+$17]. In a proximity effect the induced magnetism is driven by the CGT layer in direct contact with WTe only. Therefore, the number of layers in the CGT flakes is not a parameter that requires a precise control in our devices.
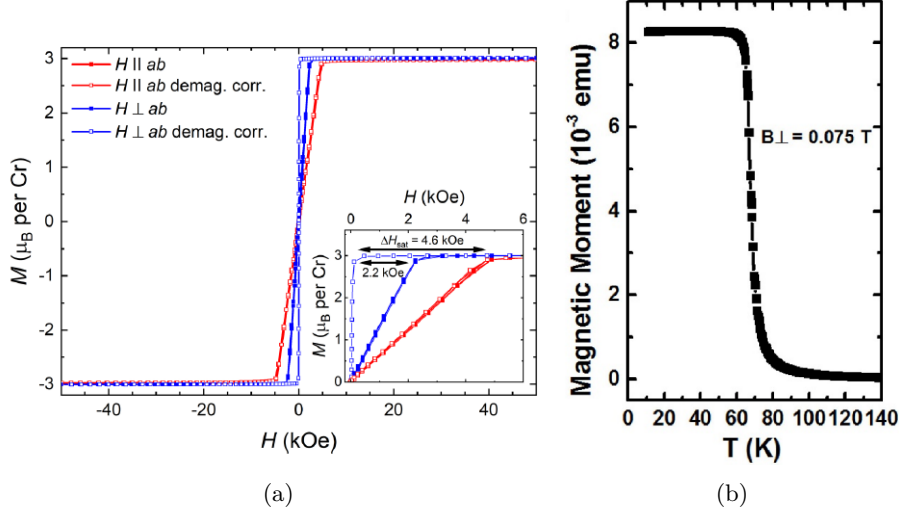
Figure 2: (a) Characterization of the magnetization of CGT as a function of out-of-plane (blue) and in-plane (red) fields, with (filled symbols) and without (open symbols) corrections for the contributions of shape anisotropy, by means of SQUID magnetometry. The conclusion is that the magnetocrystaline anisotropy is out-of-plane and the coercive field is negligible. *Source: S. Selter, G. Bastien, A. U. B. Wolter, S. Aswartham, and B. Büchner (Jan 2020)Magnetic anisotropy and low-field magnetic phase diagram of the quasi-two-dimensional ferromagnet $Cr_2Ge_2Te_6$, Phys. Rev. B 101, 014440, 10.1103/PhysRevB.101.014440.*
(b) Temperature-dependent magnetization characterization of bulk CGT under a 0.075-T out-of-plane field, by SQUID magnetometry. The curve shows a Curie temperature of 66K. *Source: Gong, C., Li, L., Li, Z. et al. Discovery of intrinsic ferromagnetism in two-dimensional van der Waals crystals. Nature 546, 265–269 (2017). https://doi.org/10.1038/nature22060*

2.2   The Anomalous Hall effect as an indicator of magnetic order

The Anomalous Hall effect (AHE) is an electrical transport phenomenon occurring in solids with broken time reversal symmetry, such as ferromagnets. It was first discovered in the 1880s by Edwin H. Hall in experiments in Nickel and Cobalt [Ph.81], and it has since become an experimental signature of magnetic order in materials.

The transversal resistance (also called the Hall resistance) in a magnetic conductor subject to a magnetic field can be described by a simple phenomenological formula:

$$R_{XY} = R_O H_z + R_A M_z \tag{1}$$

The first term corresponds to the ordinary Hall effect (OHE), which can be understood in terms of the classical Lorentz force acting on the moving charges. For electron carriers the ordinary Hall coefficient can be expressed as $R_O = \frac{1}{e \cdot n}$, where e is the elementary charge and n the carrier density. The second term corresponds to the AHE, and its theoretical understanding has been a challenge for more than a century. With the discovery of the importance of the Berry phase and incorporation of intrinsic band effects to the picture, it is now accepted that the origin of the AHE is a combination of extrinsic and intrinsic effects. Extrinsic effects correspond to different scattering mechanisms, such as the spin-dependent skew scattering and the side-jump mechanism, while intrinsic effects are a consequence of the anomalous velocity acquired by the carries, which has its origin in the Berry curvature [NSO$^+$10].

The OHE is present in all conductors, whereas the AHE is only present in magnetic materials, in which a spontaneous Hall current exists even in the absence of a magnetic field. Even if the nature of coefficients R_O and R_A is material depended, for a wide range of magnetic metals they are linear. In that case the resistance R_{XY} as a function of magnetic field follows the magnetization M_z, characterized by a hysteretic behaviour below a certain coercive field H_C, plus a constant slope coming from the OHE.

The AHE offers the possibility to identify magnetic order in a material using only transport measurements, which makes it experimentally convenient. That is exactly the role of the AHE in the proximity experiments carried out during the master thesis. A current will be passed though the originally non-magnetic WTe_2, and since the adjacent the magnetic layer (CGT) is expected to be highly insulating, the existence of AHE signal will be an indication of proximity-induced magnetic order in WTe_2. Temperature dependent measurements of the Hall resistance will be carried out, expecting that for $T > T_C$, the CGT is non-magnetic and therefore, R_{XY} in WTe_2 is given by the ordinary Hall effect. For $T < T_C$, i.e., when CGT becomes magnetic, R_{XY} in WTe_2 should present the ordinary Hall effect together with an anomalous Hall signal.

3 Methodology

This section will explain the steps of the device fabrication process and present the experimental setup.

3.1 Device fabrication

The device fabrication process can be broken down to the following steps.

3.1.1 Exfoliation of 2D materials

The fabrication process starts with the mechanical exfoliation of the van der Waals materials that will form the heterostructure. The mechanical exfoliation follows the 'scotch-tape' method [GLQ$^+$18], in which the source material is peeled-off using an adhesive tape. The exfoliated material is then transferred from the tape onto an insulating substrate. In this thesis we have p-doped Si coated with 440 nm SiO_2 as the supporting substrate. The flakes are localized on the substrate using an optical microscope, which enables to estimate the thickness of the exfoliated flakes by optical contrast and the analysis of the red-green-blue channels.
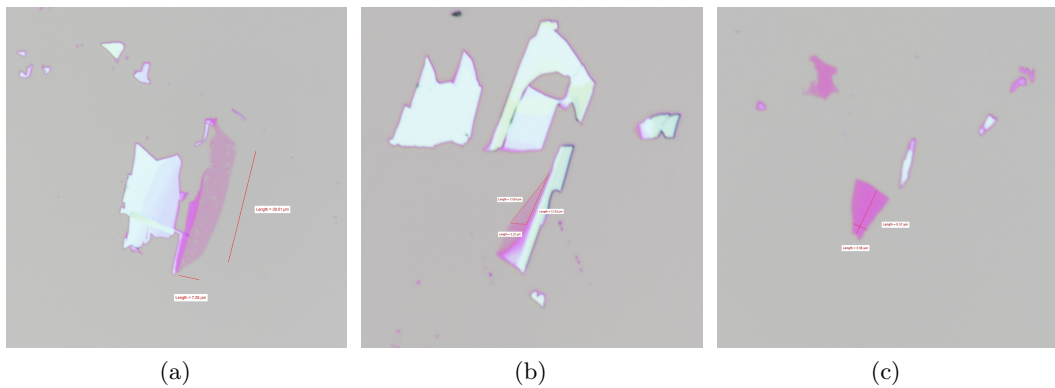
Figure 3: Examples of WTe_2 flakes.

(a)　　　　　　　　　　(b)　　　　　　　　　　(c)
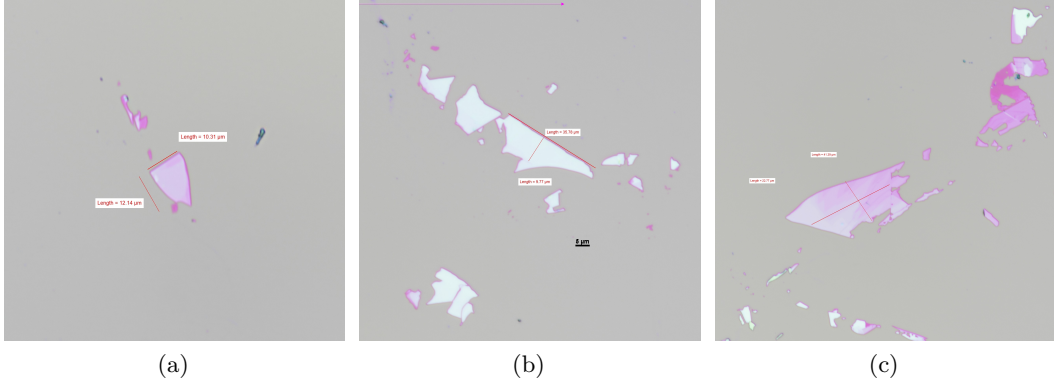
Figure 4: Examples of CGT flakes.

Remarkably, the exfoliation process was carried out in a glove box. The glove bow allows to realize the exfoliation process in a control atmosphere of Ar with very low concentrations of O_2 and H_2O (below 1 p.p.m) in order to prevent oxidation of air-sensitive materials, such as WTe_2. We targeted WTe_2 flakes of about $6\mu m \times 3\mu m$ in size and 10-50 nm thickness. It is worth to note that exfoliation of thin enough WTe_2 with the required dimensions is particularly challenging and limited in yield. Figure 3 shows optical images of some of the exfoliated flakes that were used in the final devices.

In the case of CGT, the exfoliated flakes must be larger in size than the WTe_2 flake, so that when stacked on top of WTe_2, it protects against oxidation, and their thickness is not relevant, which made the process considerably easier than for WTe_2. Figure 4 show optical images of some of the exfoliated CGT flakes.

3.1.2　E-beam lithography and evaporation of Hall bar contacts

We minimized the number of chemicals and lithography steps on the exfoliated crystals. Therefore, we have first designed and fabricated the contacts using electron beam lithography, and then transferred the van der Waals heterostructure on top of them using deterministic transfer methods. The devices are based on a Hall bar geometry, which include longitudinal and transversal contacts as shown in Figure 5. The Hall bar consists of six contacts, two of them define a long channel and are used for current bias (1 and 4 in the image). The other four contacts are designed in the sides and used to measure either the longitudinal (2-3 and 5-6) or the transverse voltage (2-6 and 3-5). Using four probes eliminates measurement errors due to the probe resistance and the contact resistance between each metal probe and the heterostructure.

The pre-patterned Hall bars have been fabricated on a 440 nm SiO_2 substrate that is previously cleaned with an O_2 plasma. We then spin-coat a polymer layer made of a bilayer of methyl-methacrylate (MMA) and polymethyl-methacrylate (PMMA). The polymer is then exposed to electrons using an e-beam lithography system. After lithography, the chip is soaked in a chemical development Methyl-isobutyl-ketone (MBIK) diluted in isopropanol. Finally, the chip is dried with N_2. The e-beam lithography is followed by the metallization of the contacts. We have used e-beam evaporation of 5 nm of Ti and 30nm of Pd. The evaporation is then followed by a lift off in acetone. Figure 5 shows an optical image of the final contacts, onto which the WTe_2/CGT stack will be transferred.
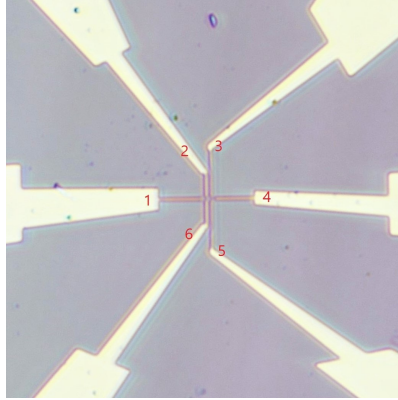
Figure 5: Electrodes in Hall bar geometry.

3.1.3   Heterostructure stacking and deterministic transfer onto the pre-patterned contacts

In order to fabricate van der Waals heterostructure, we have used deterministic transfer and pick-up techniques [PGJ$^+$16]. The schematics of the process are shown in Figure 6. First, we pick-up the CGT flake previously exfoliated onto the SiO$_2$ substrate using a viscoelastic stamp. The viscoelastic stamp is composed of Polydimethylsiloxane (PDMS) coated with a layer of Polycarbonate (PC). The stamp is attached to a glass slide and mounted in a x, y, z micromanipulator, which allows us to precisely control the position of the stamp respect to the targeted flake that is mounted in the heated optical microscope stage. The pick-up of the CGT flake is realized by heating the stage up to T = 120 ºC. In the second step, the chip with WTe_2 is mounted on the microscope stage and picked up with the CGT flake previously transferred to the PDMS/PC stamp. The whole stack is then transferred on top of the pre-patterned Hall bar contacts. This last transfer is done at T = 200 ºC to detach the PC from the PDMS. The whole device is soaked in chloroform and IPA to remove the melted PC.
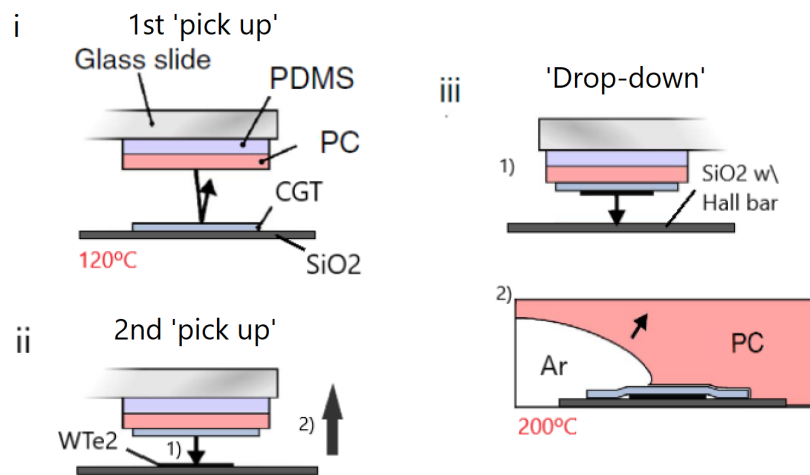
Figure 6: Scheme of the stacking and transfer. *Adapted from: Pizzocchero, F., Gammelgaard, L., Jessen, B. et al. The hot pick-up technique for batch assembly of van der Waals heterostructures. Nat Commun 7, 11894 (2016). https://doi.org/10.1038/ncomms11894.*

3.1.4 High vacuum annealing

The last step before starting the measurement process is to anneal the device in high vacuum at a specific temperature, for a given time span. The annealing process is a common step that will create a better interface between CGT and WTe2 and between the WTe_2 and Pd contacts. The annealing temperature must be chosen so that the constituent materials do not suffer any degradation. In the case of CGT/WTe_2 we have observed degradation of WT_2 above 280 ºC, so that we have started with annealing temperatures of 200ºC.

3.2 Experimental set-up

The device is fixed to a chip carrier and wire-bonded for electrical connections. The magneto-transport measurements were carried out with a lock-in (Standford Research System) at frequencies f_{ac}= 177 Hz in a closed cycle cryostat with a base temperature of T_{base} = 6 K. Current ac bias was carried out with a Keithley current source (Model 6221). In order to avoid sample damage, the amplitude of the ac current was chosen to account for the different resistances of the devices. The magneto-transport setup includes an electro-magnet (GMW) with magnetic fields up to 0.6 T with variable orientation from out of plane to in-plane magnetic fields.

4 Results and discussion

In this section the obtained results will be presented and discussed in chronological order. The study started with interesting results from a WTe_2/CGT device, that could possibly be attributed to a proximity effect, but showed unexpected magnetic properties that deviated from the ones expected for CGT. The results made us suspect that the high vacuum annealing treatment was causing alterations in the magnetic material. At this point, the investigation turned into a dedicated study of CGT, and a device composed only of CGT was fabricated and characterized to gain a better understanding of the observed phenomena. We found that the sample processing altered both the magnetic and transport properties of CGT, causing an increase of the T_c, magnetic anisotropy, and electrical conductivity. The findings discarded the possibility that a magnetic proximity effect had been observed in the heterostructure. In turn, we have discovered a new approach to significantly enhance the magnetic properties of CGT. The underlying mechanism for the observed phenomena is still not fully understood. However, a dramatic drop in the resistance indicates that the annealing leads to CGT doping. Comparison with prior theoretical work and experiments with ionic gating seems to suggest that doping could be linked to the changes in the magnetic properties.

4.1 Heterostucture device

Figure 7 shows the device fabricated for the WTe_2/CGT heterostructure. With the aim of creating better contact between the device and the pre-pattern contacts, we carried out an annealing treatment. Moreover, as mentioned in Section 3.1.4, the annealing process is also a common step introduced in the fabrication to improve the interface quality between van der Waals materials.

<table>
<tr><td>(a) 10x</td><td>(b) 100x</td></tr>
</table>
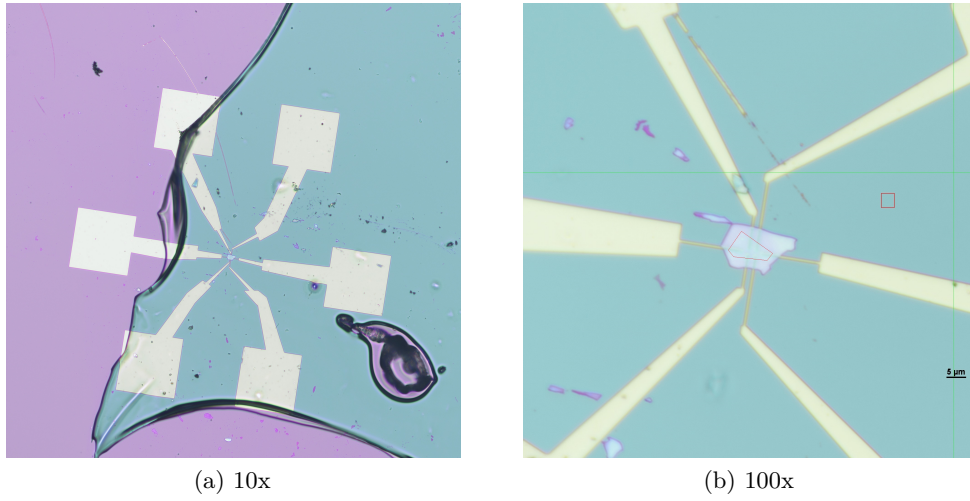
Figure 7: Images of the heterostructure device at different amplitudes, with the melted polymer used for the transfer on top. The red line frames the WTe_2 flake underneath the CGT.

4.1.1 Magneto-transport measurements after annealing at T_{an}= 200 ºC

The first annealing process was carried out at annealing temperature T_{an}= 200 ºC for three hours in high vacuum. We first measured the longitudinal resistance R_{XX} as a function of temperature (Figure 8) that shows an increase of resistance with temperature as expected from metallic or semi-metallic samples, compatible with WTe_2. We followed with magneto-transport measurements in order to observe the proximity-induced magnetism. Both R_{XX} and R_{XY} were measured as a function of out-of-plane magnetic field B at different temperatures, above and below the reported Curie temperature of pristine CGT T_C= 66 K.
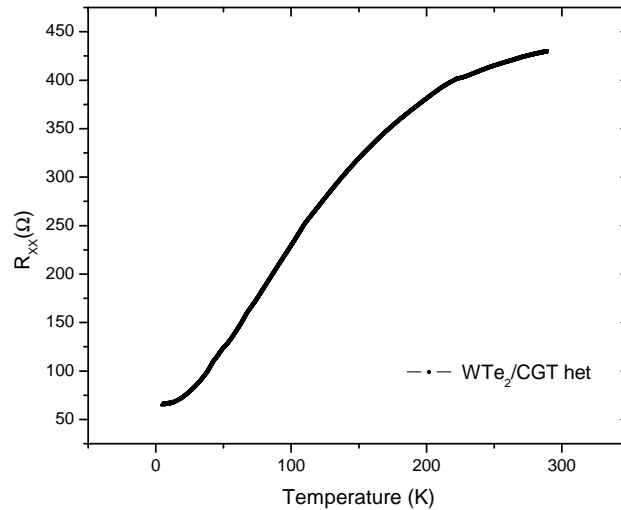
Figure 8: Temperature dependence of R_{XX}.
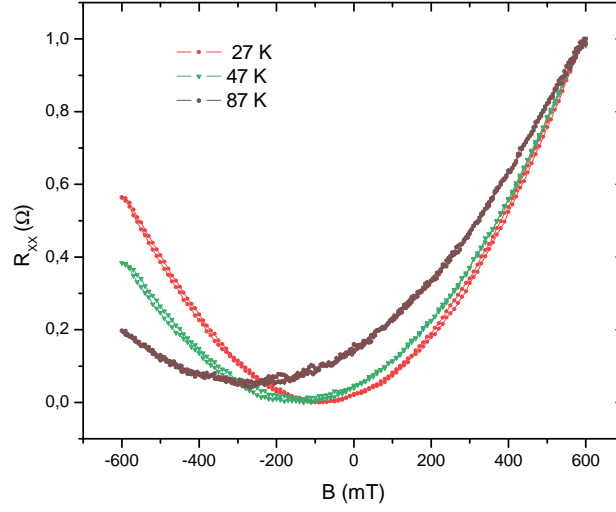
Figure 9: Magnetoresistance as a function of out-of-plane magnetic field for temperatures below and above T_c=66K. The curves have been normalized in order to show the parabolic shape. For raw data go to Appendix C

.
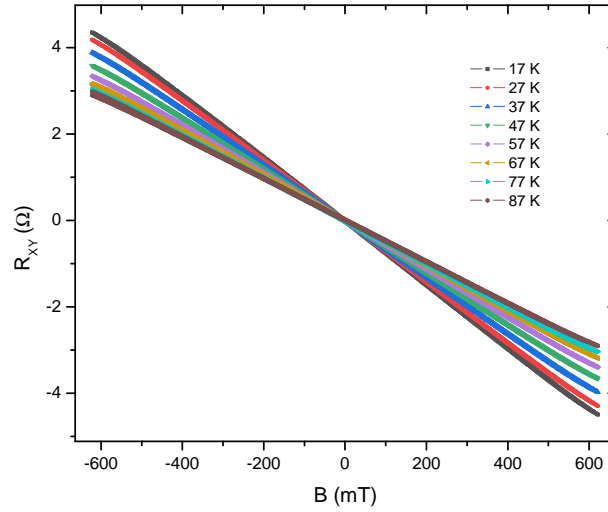
Figure 10: Hall resistance as a function of out-of-plane magnetic field at different temperatures.

Figure 10 shows R_{XY} vs. out of plane magnetic field at different temperatures above and below T_C, from which we observe ordinary Hall effect without any signature of AHE. The change in the slope of curves with temperature is associated to a slight increase in carrier density with increasing temperatures that stems from the semi-metallic character of WTe_2. Similar behaviour was observed in previous magneto-transport measurements in few-layers WTe_2 samples during my internship period. From these results we conclude that the magneto-transport measurement does not show any signatures of magnetic proximity effect on the WTe_2 layer. Figure 9 shows R_{XX} vs. out-of-plane magnetic field at different

temperatures. The observed parabolic dependence stems from the semi-metallic nature of WTe_2 [ZLY$^+$15] and was also verified during my internship in few layer WTe_2 samples. The noticeable tilt of the parabolas for higher temperatures is due to the linear contribution of the Hall signal. The obtained results for the WTe_2 devices are included in Appendix A for comparison.

4.1.2 Magneto-transport measurements after annealing at T_{an}= 280ºC

We carried out a second annealing process in the same at a higher temperature of T_{an}= 280ºC for five hours in high vacuum. The aim of increasing the annealing temperature is to create a higher quality van der Waals interface between CGT and WTe_2.

First, we measured temperature dependence of R_{XX}, which shows an increase with temperature reflecting again the semi-metallic behaviour of the sample (included in Appendix B). Remarkably, after the second annealing treatment, we observed a dramatic change of the device behaviour at low temperatures. Figure 11 shows magneto-transport measurements of R_{XY} as a function of out-of-plane magnetic field that show clear anomalous Hall hysteresis loops. Unlike the magnetic behaviour of CGT, the anomalous Hall signal persists up to T_c= 100 K in our samples, which correspond to a 50% increase from the expected T_c= 66 K for bulk CGT. Furthermore, the measured hysteresis loops have coercive fields of about 100 mT at 10K, which is in stark contrast with the negligible H_c observed in CGT. We also carried out measurements of the Hall resistance R_{XY} at different magnetic field orientations, from out-of-plane to in-plane, which clearly show the perpendicular magnetic anisotropy of CGT. These results can be found in Appendix B.

Besides, magneto-resistance measurements present parabolic behaviour with an anti-symmetric component in R_{XX} at $\pm H_C$ as shown in Fig. 12. The physical mechanism that gives rise to these magnetic anomalies is still unclear, since all expected magneto-resistance mechanisms would lead to an even response with magnetic field.
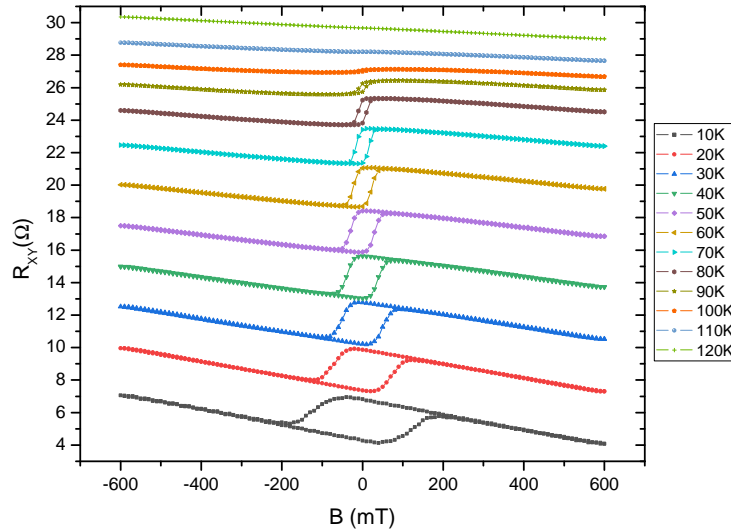
Figure 11: Hall resistance as a function of out-of-plane magnetic field for different temperatures. The curves are plotted with an offset, for raw data go to Appendix C
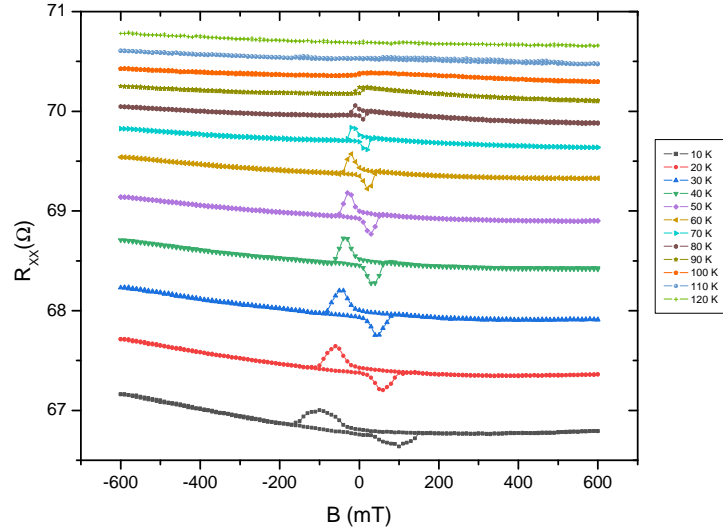
Figure 12: Magnetoresistance as a function of out-of-plane magnetic field at different temperatures. The curves are plotted with an offset, for raw data go to Appendix C.

In summary, the sample exhibits very different magneto-transport behaviour after the second annealing at 280ºC, displaying clear signatures of magnetism. The magneto-transport measurements suggest a change in the magnetic response of CGT, particularly, we observe a significant increase of magnetic anisotropy and T_c respect to the reported values in pristine CGT samples. One could infer the possibility that annealing temperatures might alter the properties of CGT such as its doping level. However, the mechanism in which the annealing influences their magnetic properties is still unclear. In this regard, similar results including both the increase in anisotropy and a 130% enhancement in T_c, have been reported in CGT when adjacent to a tungsten layer [ZSH+21]. Such large enhancement is attributed to interfacial W-Te chemical bonding between the tungsten layer and the tellurium in the CGT. Indeed, the same interfacial bonding could appear between the tungsten of WTe_2 and the tellurium of CGT in our samples. However, such interfacial effect, occurring only in a few layers of the constituent materials, should not alter dramatically the bulk properties of CGT. We note that in the case of CGT/tungsten samples, authors carried out annealing treatments at temperatures as high as 400 K and claimed no structural damage of the CGT.

The fact that annealing process influences the CGT behaviour is critical to clearly discern whether the observed anomalous Hall hysteresis loop arises from proximity-induced effect in the WTe_2. For instance, if CGT changes its semiconducting behaviour and becomes conducting, e.g. due to a change of its doping level, the current running in the WTe_2 layer would be shunted by the CGT and thus, the observed AHE would arise from the CGT itself. Therefore, we also carried out similar magneto-transport experiments in CGT subject to different annealing temperatures. These experiments are indeed essential to interpret the current results as AHE induced by magnetic proximity effects.

4.2 CGT device

We fabricated a sample consisting solely of CGT following the same fabrication process than for the CGT/WTe_2 heterostructure. The device is shown in Figure 13. The same annealing treatments at 200 ⁰C and 280 ⁰C and magneto-transport experiments were carried out in the CGT sample.
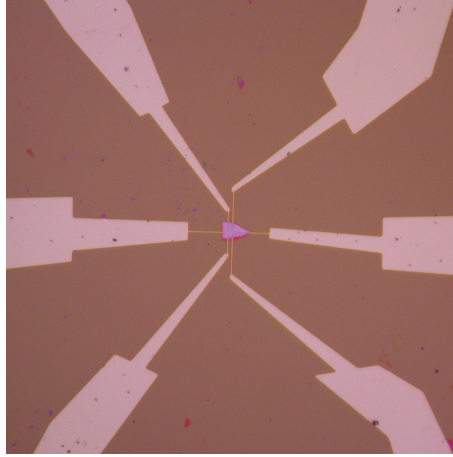
Figure 13: CGT device at 50x magnification

4.2.1 Transport measurements on the pristine sample

The first measurements were carried out in the pristine sample without any annealing treatment. Figure 14 shows R_{XX} as a function of temperature, which clearly demonstrates the semi-conducting behaviour of CGT with resistance values in the order of 400kΩ and of 1.4 MΩ at room temperature and around 250K (the lowest temperature measured), respectively.
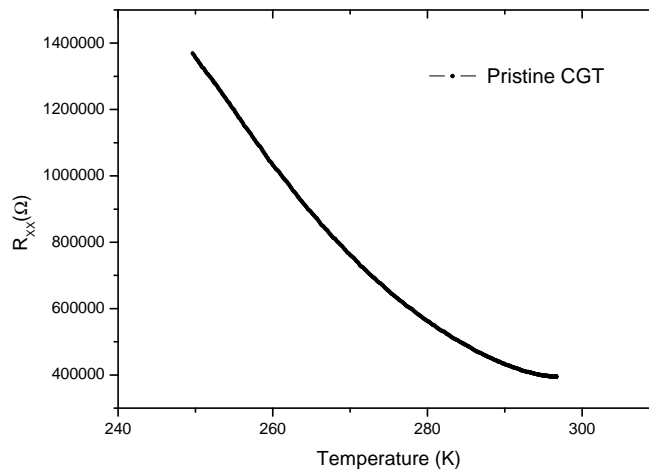
Figure 14: Temperature dependence of the pristine CGT device.

4.2.2 Magneto-transport measurements of the annealed sample

After annealing at 200ºC and 280ºC, we observe an overall decrease of the sample resistance as well as change in the R_{XX} vs. temperature. As shown in Fig. 15, R_{XX} is the order of 10s of kilo Ohms, which is orders of magnitude lower than the resistance values measured in the pristine sample. The resistance decreases with the decreasing temperature, and starts to increase below T= 90K, which indicates a strong deviation from the expected semiconducting behaviour.
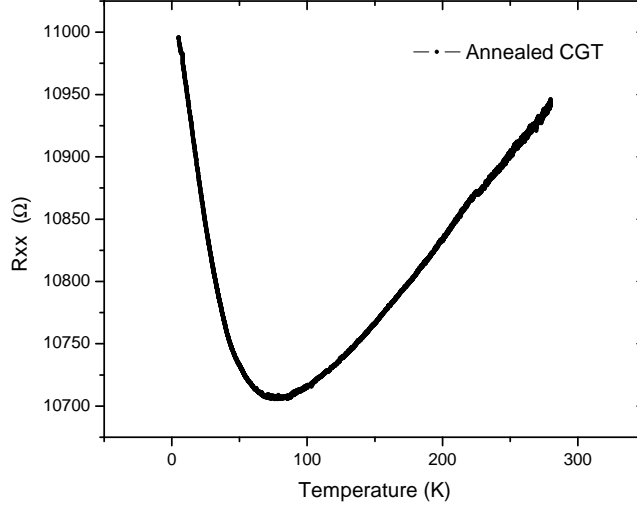
Figure 15: Temperature dependence of R_{XX} after the annealings.

The low resistance values allowed us to perform magneto-transport measurements in the CGT device. We followed the same procedure as for the heterostructure sample and carried out measurements of R_{XX} and R_{XY} as a function of the out-of-plane magnetic field. The results are shown in Figure 16. Firstly, the Hall hysteresis loops display the same enhancement on the magnetic anisotropy, with coercive fields of about 100 mT at 10K. Secondly, the same enhancement of 50% on the T_c is observed, with anomalous Hall signals prevailing up to 100K. Thirdly, R_{XX} exhibits the same antisymmetric anomalies as the ones observed in CGT/WTe_2, but with opposite sign. The results clearly demonstrated that the current is flowing through CGT in the WTe_2/CGT heterostructure after the 280ºC annealing.

4.3 Discussion

From the experiments carried out in CGT samples, it is clear that annealing treatments influences its transport properties, in particular CGT becomes conducting. This key experiment, overlooked in most of the reported works, has strong consequences on the interpretation of the results. It is not possible to conclude that the anomalous Hall signal observed in the van der Waals heterostructures stems from proximity-induced magnetism but from shunting of the current trough the CGT layer.

It has been reported that the increase in magnetic anisotropy and T_c can be controlled by electrostatic gating, where heavy doping promotes a double-exchange mechanism that is mediated by free carriers, which dominates over the superexchange mechanism of the
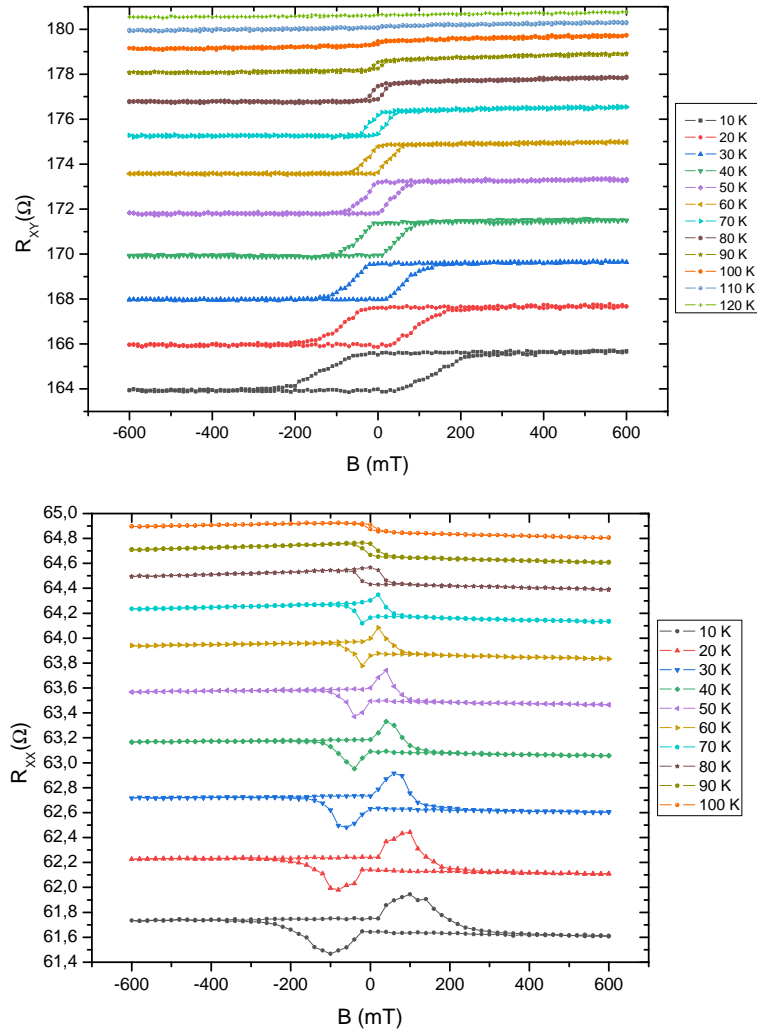
Figure 16: Results of magneto-transport measurements at different temperatures for the annealed CGT device. The curves are plotted with an offset, for raw data go to Appendix C

original insulating state [VKC⁺20]. We believe that during annealing, Te atoms evaporate due to the high volatility of this element. Such evaporation results in impurities and vacancies that heavily dope the material and make it conducting, as well as enhance the magnetic anisotropy and Curie temperature of the material.

Th mechanism that gives rise to the antisymmetric effect on the longitudinal magnetor-resistance has to be yet understood. We note that the geometry of the samples is not ideal (see figure 13), and the current distribution across the samples might be inhomogeneous. Such inhomogeneous current results in contributions to R_{XX} from transversal RXY voltages. To further explore this effect, it is necessary to fabricate samples with well-defined channel widths. Currently, we are carrying out magneto-transport experiments in CGT samples with optimal lateral geometry and contact configuration. Here, rectangular CGT flakes are selected from the exfoliation process, and contacts are defined on top of the flake in a Hall bar geometry.

5 Conclusions and next steps

In conclusion, we have observed that high vacuum annealing treatment at T_{an}=200 ºC for 3 hours plus at T_{an}=280 ºC for 5 hours resulted in a significant increase of magnetic anisotropy and T_c of van der Waals ferromagnet CGT. The coercive field has increased form negligible for pristine CGT to H_c=100 mT at 10 K, and the Curie temperature has presented a 50% enhancement from T_c=66 K to T_c=100K. Additionally, the annealing process also results in a remarkable increased conductivity in CGT that opens the possibility to study it magnetic properties via transport measurements. As consequence, the observed AHE effect in the annealed WTe_2/CGT device cannot be interpreted as proximity-induced magnetic order on WTe_2, but the signal coming from the conducting CGT.

The set of experiments carried out during the master thesis have demonstrated the importance of making simple characterization tests before integrating the materials in an heterostructure. Currently, this tests are sometimes lacking in the field, with many one device papers claiming complex emerging phenomena without testing the constituent elements separately. Take as example the aforementioned study where the increase in anisotropy and T_c in annealed devices is attributed to an interface effect [ZSH$^+$21], without performing the simple test we have carried out. The obtained results have been an important lesson to keep in mind in the search for magnetic proximity effects in van der Waals heterostructures.

More characterization of the device is needed to complete the understanding of the progressive alterations. Firstly, a TEM image of a cross-section of the first CGT device should be performed to see if there is structural damage. In van der Waals materials, TEM images display very clear images of the layered structure, and any diffusion can be clearly visible.

Secondly, the magnetization of the CGT should be monitored by direct measurements, such as a SQUID magnetometer, to compare it to the magneto-transport results. This would give a direct prove of the increase of the magnetic anisotropy and T_c.

Finally, after a complete understanding of the CGT behaviour is achieved, the study of the WTe_2/CGT heterostructures should resume, only performing annealing treatments that do not alter the CGT. The in-depth understanding of the transport properties of CGT would make any sign of magnetism a convincing prove of induced magnetism in WTe_2, which would be a big step forward the realization of the QAHE in a van der Waals heterostructure.

Bibliography

[AXF⁺14] Mazhar N. Ali, Jun Xiong, Steven Flynn, Jing Tao, Quinn D. Gibson, Leslie M. Schoop, Tian Liang, Neel Haldolaarachchige, Max Hirschberger, N. P. Ong, and R. J. Cava. Large, non-saturating magnetoresistance in wte2. *Nature*, 514(7521):205–208, September 2014.

[BAG⁺21] Semonti Bhattacharyya, Golrokh Akhgar, Matthew Gebert, Julie Karel, Mark T. Edmonds, and Michael S. Fuhrer. Recent progress in proximity coupling of magnetism to topological insulators. *Advanced Materials*, 33(33):2007795, June 2021.

[CZF⁺13] Cui-Zu Chang, Jinsong Zhang, Xiao Feng, Jie Shen, Zuocheng Zhang, Minghua Guo, Kang Li, Yunbo Ou, Pang Wei, Li-Li Wang, Zhong-Qing Ji, Yang Feng, Shuaihua Ji, Xi Chen, Jinfeng Jia, Xi Dai, Zhong Fang, Shou-Cheng Zhang, Ke He, Yayu Wang, Li Lu, Xu-Cun Ma, and Qi-Kun Xue. Experimental observation of the quantum anomalous hall effect in a magnetic topological insulator. *Science*, 340(6129):167–170, 2013.

[CZK⁺15] Cui-Zu Chang, Weiwei Zhao, Duk Y. Kim, Haijun Zhang, Badih A. Assaf, Don Heiman, Shou-Cheng Zhang, Chaoxing Liu, Moses H. W. Chan, and Jagadeesh S. Moodera. High-precision realization of robust quantum anomalous hall state in a hard ferromagnetic topological insulator. *Nature Materials*, 14(5):473–477, March 2015.

[DSC⁺19] P K Das, D Di Sante, F Cilento, C Bigi, D Kopic, D Soranzio, A Sterzi, J A Krieger, I Vobornik, J Fujii, T Okuda, V N Strocov, M B H Breese, F Parmigiani, G Rossi, S Picozzi, R Thomale, G Sangiovanni, R J Cava, and G Panaccione. Electronic properties of candidate type-ii weyl semimetal wte2. a review perspective. *Electronic Structure*, 1(1):014003, March 2019.

[DYS⁺20] Yujun Deng, Yijun Yu, Meng Zhu Shi, Zhongxun Guo, Zihan Xu, Jing Wang, Xian Hui Chen, and Yuanbo Zhang. Quantum anomalous hall effect in intrinsic magnetic topological insulator mnbi2te4. *Science*, 367(6480):895–900, 2020.

[GKMN19] M. Gibertini, M. Koperski, A. F. Morpurgo, and K. S. Novoselov. Magnetic 2d materials and heterostructures. *Nature Nanotechnology*, 14(5):408–419, May 2019.

[GLL⁺17] Cheng Gong, Lin Li, Zhenglu Li, Huiwen Ji, Alex Stern, Yang Xia, Ting Cao, Wei Bao, Chenzhe Wang, Yuan Wang, Z. Q. Qiu, R. J. Cava, Steven G. Louie, Jing Xia, and Xiang Zhang. Discovery of intrinsic ferromagnetism in two-dimensional van der waals crystals. *Nature*, 546(7657):265–269, April 2017.

[GLQ⁺18] Enlai Gao, Shao-Zhen Lin, Zhao Qin, Markus J. Buehler, Xi-Qiao Feng, and Zhiping Xu. Mechanical exfoliation of two-dimensional materials. *Journal of the Mechanics and Physics of Solids*, 115:248–262, 2018.

[GPB⁺96] S. Guéron, H. Pothier, Norman O. Birge, D. Esteve, and M. H. Devoret. Superconducting proximity effect probed on a mesoscopic length scale. *Physical Review Letters*, 77(14):3025–3028, September 1996.

[Hal88] F. D. M. Haldane. Model for a quantum hall effect without landau levels: Condensed-matter realization of the "parity anomaly". *Phys. Rev. Lett.*, 61:2015–2018, Oct 1988.

[JFS21] Roland K. Kawakami Stephan Roche Sergio O. Valenzuela Juan F. Sierra, Jaroslav Fabian. Van der waals heterostructures for spintronics and opto-spintronics. *Phys. Rev. Lett.*, 16, Aug 2021.

[LH21] Jieyi Liu and Thorsten Hesjedal. Magnetic topological insulator heterostructures: A review. *Advanced Materials*, page 2102427, October 2021.

[LWH+17] Peng Li, Yan Wen, Xin He, Qiang Zhang, Chuan Xia, Zhi-Ming Yu, Shengyuan A. Yang, Zhiyong Zhu, Husam N. Alshareef, and Xi-Xiang Zhang. Evidence for topological type-II weyl semimetal wte2. *Nature Communications*, 8(1), December 2017.

[MOP+17] Sajedeh Manzeli, Dmitry Ovchinnikov, Diego Pasquier, Oleg V. Yazyev, and Andras Kis. 2d transition metal dichalcogenides. *Nature Reviews Materials*, 2(8), June 2017.

[MW66] N. D. Mermin and H. Wagner. Absence of ferromagnetism or antiferromagnetism in one- or two-dimensional isotropic heisenberg models. *Phys. Rev. Lett.*, 17:1133–1136, Nov 1966.

[NSO+10] Naoto Nagaosa, Jairo Sinova, Shigeki Onoda, A. H. MacDonald, and N. P. Ong. Anomalous hall effect. *Rev. Mod. Phys.*, 82:1539–1592, May 2010.

[OKB+19] M. M. Otrokov, I. I. Klimovskikh, H. Bentmann, D. Estyunin, A. Zeugner, Z. S. Aliev, S. Gaß, A. U. B. Wolter, A. V. Koroleva, A. M. Shikin, M. Blanco-Rey, M. Hoffmann, I. P. Rusinov, A. Yu. Vyazovskaya, S. V. Eremeev, Yu. M. Koroteev, V. M. Kuznetsov, F. Freyse, J. Sánchez-Barriga, I. R. Amiraslanov, M. B. Babanly, N. T. Mamedov, N. A. Abdullayev, V. N. Zverev, A. Alfonsov, V. Kataev, B. Büchner, E. F. Schwier, S. Kumar, A. Kimura, L. Petaccia, G. Di Santo, R. C. Vidal, S. Schatz, K. Kißner, M. Ünzelmann, C. H. Min, Simon Moser, T. R. F. Peixoto, F. Reinert, A. Ernst, P. M. Echenique, A. Isaeva, and E. V. Chulkov. Prediction and observation of an antiferromagnetic topological insulator. *Nature*, 576(7787):416–422, December 2019.

[PGJ+16] Filippo Pizzocchero, Lene Gammelgaard, Bjarke S. Jessen, José M. Caridad, Lei Wang, James Hone, Peter Bøggild, and Timothy J. Booth. The hot pick-up technique for batch assembly of van der waals heterostructures. *Nature Communications*, 7(1), June 2016.

[Ph.81] E.H. Hall Ph.D. Xviii. on the "rotational coefficient" in nickel and cobalt. *The London, Edinburgh, and Dublin Philosophical Magazine and Journal of Science*, 12(74):157–172, 1881.

[SBW+20] S. Selter, G. Bastien, A. U. B. Wolter, S. Aswartham, and B. Büchner. Magnetic anisotropy and low-field magnetic phase diagram of the quasi-two-dimensional ferromagnet cr2ge2te6. *Phys. Rev. B*, 101:014440, Jan 2020.

[TZW+17] Shujie Tang, Chaofan Zhang, Dillon Wong, Zahra Pedramrazi, Hsin-Zon Tsai, Chunjing Jia, Brian Moritz, Martin Claassen, Hyejin Ryu, Salman Kahn, Juan Jiang, Hao Yan, Makoto Hashimoto, Donghui Lu, Robert G. Moore, Chan-Cuk Hwang, Choongyu Hwang, Zahid Hussain, Yulin Chen, Miguel M. Ugeda, Zhi Liu, Xiaoming Xie, Thomas P. Devereaux, Michael F. Crommie, Sung-Kwan Mo, and Zhi-Xun Shen. Quantum spin hall state in monolayer 1t'-wte2. *Nature Physics*, 13(7):683–687, June 2017.

[VKC+20] Ivan A. Verzhbitskiy, Hidekazu Kurebayashi, Haixia Cheng, Jun Zhou, Safe Khan, Yuan Ping Feng, and Goki Eda. Controlling the magnetic anisotropy in cr2ge2te6 by electrostatic gating. *Nature Electronics*, 3(8):460–465, June 2020.

[WYH+15] Hongming Weng, Rui Yu, Xiao Hu, Xi Dai, and Zhong Fang. Quantum anomalous hall effect and related topological electronic states. *Advances in Physics*, 64(3):227–282, 2015.

[ZLY+15] Yanfei Zhao, Haiwen Liu, Jiaqiang Yan, Wei An, Jun Liu, Xi Zhang, Huichao Wang, Yi Liu, Hua Jiang, Qing Li, Yong Wang, Xin-Zheng Li, David Mandrus,

X. C. Xie, Minghu Pan, and Jian Wang. Anisotropic magnetotransport and exotic longitudinal linear magnetoresistance in wte2 crystals. *Physical Review B*, 92(4), jul 2015.

[ZRF⁺21] Wenjin Zhao, Elliott Runburg, Zaiyao Fei, Joshua Mutch, Paul Malinowski, Bosong Sun, Xiong Huang, Dmytro Pesin, Yong-Tao Cui, Xiaodong Xu, Jiun-Haw Chu, and David H. Cobden. Determination of the spin axis in quantum spin hall insulator candidate monolayer wte2. *Physical Review X*, 11(4), nov 2021.

[ZSH⁺21] Wenxuan Zhu, Cheng Song, Lei Han, Hua Bai, Qian Wang, Siqi Yin, Lin Huang, Tongjin Chen, and Feng Pan. Interface-enhanced ferromagnetism with long-distance effect in van der waals semiconductor. *Advanced Functional Materials*, 32(8):2108953, November 2021.

A   Internship period WTe_2 characterization experiments
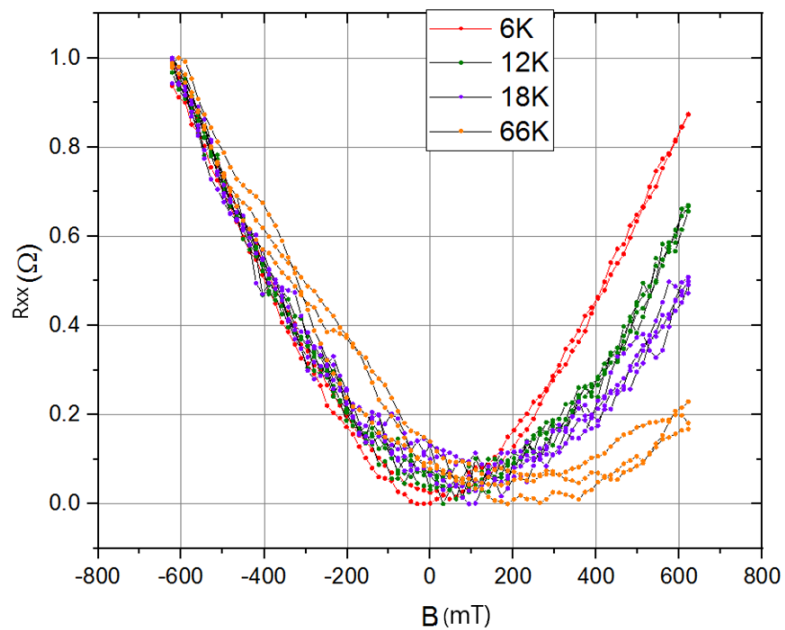
Figure 17: Parabolic magnetorresistance of the WTe_2 device characterized during the internship period.
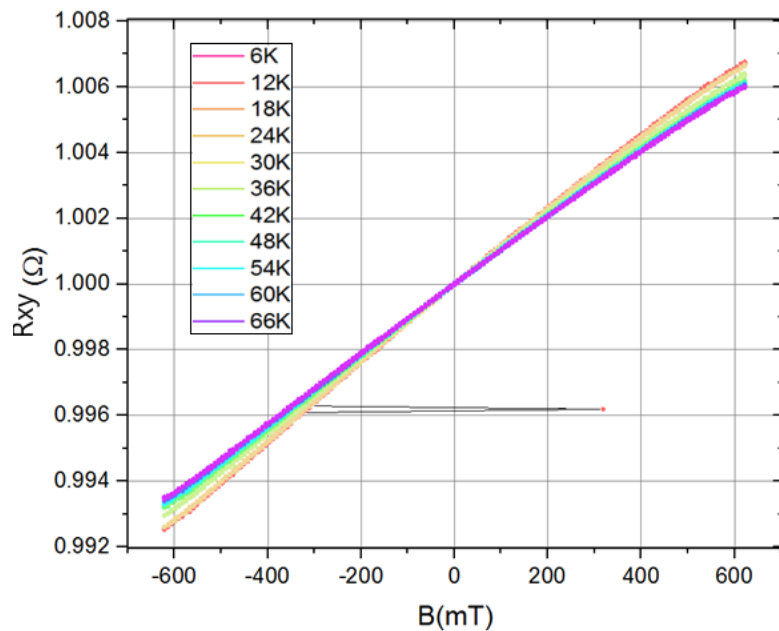
Figure 18: Hall resistance of the WTe_2 device characterized during the internship period.

B Extra characterization measurements of the WTe_2/CGT device
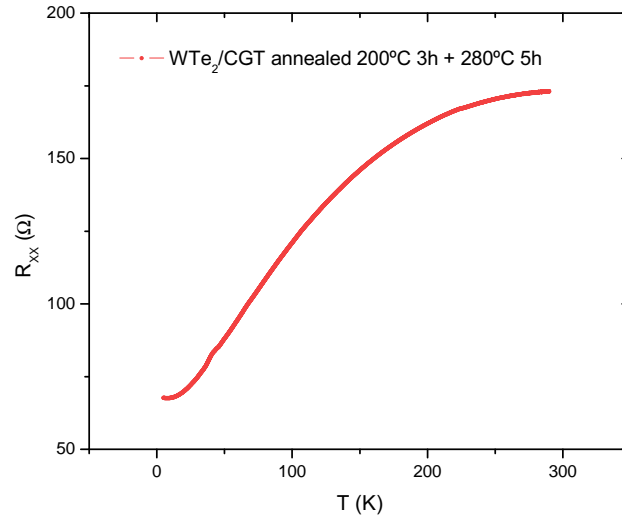
Figure 19: Temperature dependence of the heterostructure device after the second annealing. The device exhibits the same metallic behavior as before the first annealing
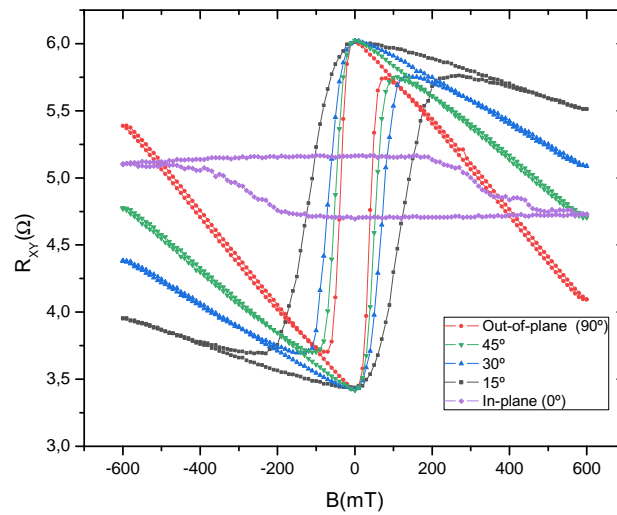
Figure 20: R_{XY} vs. magnetic field at different angles. The device shows clear out-of-plane magnetic anisotropy.

C   Raw data of the measurements presented in Section 4
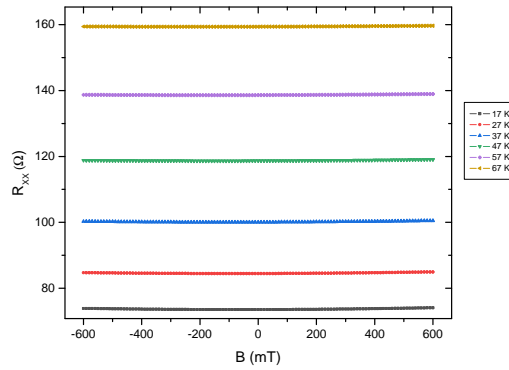
(a) Before the sencond annealing
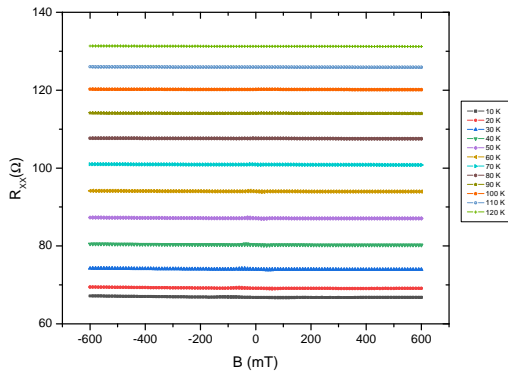
(b) After the second annealing
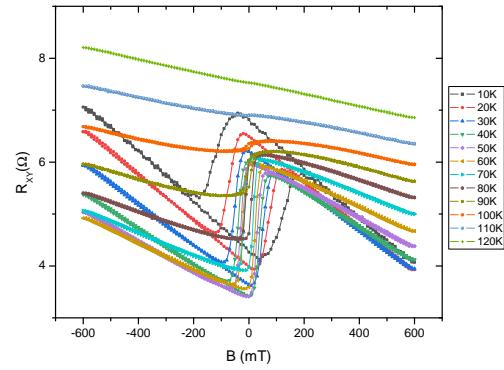
(c) After the second annealing

Figure 21: Raw data of the longitudinal and Hall resistance measurements for the heterostructure device.
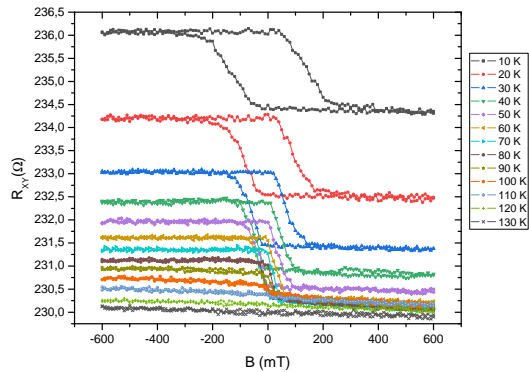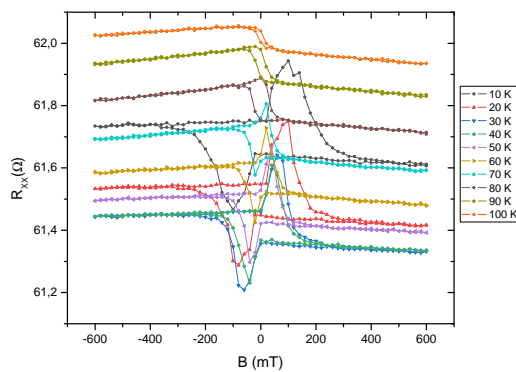
Figure 22: Raw data of the longitudinal and Hall resistance measurements for the CGT device. The Hall voltage was measured in the opposite direction as for the heterostructure, that is why it has been edited when included in the text.